IEEE Access
Multidisciplinary ⋮ Rapid Review ⋮ Open Access Journal

Received August 31, 2018, accepted September 26, 2018, date of publication October 1, 2018, date of current version October 25, 2018.

Digital Object Identifier 10.1109/ACCESS.2018.2873416

Direction-of-Arrival Estimation via Coarray With Model Errors

RUI LU[1], MING ZHANG[1], XIAOBO LIU[1], XIAOMING CHEN[1,2], (Member, IEEE), AND ANXUE ZHANG[1]

[1]School of Electronic and Information Engineering, Xi'an Jiaotong University, Xi'an 710049, China
[2]State Key Laboratory of Millimeter Waves, Nanjing 210096, China

Corresponding author: Xiaoming Chen (xiaoming.chen@mail.xjtu.edu.cn)

This work was supported in part by the National Natural Science Foundation under Grant 61471292, Grant 61501365, Grant 61601360, Grant 61801366, and Grant 61801368 and in part by the Open Project Program of State Key Laboratory of Millimeter Waves under Grant K201933.

ABSTRACT Direction-of-Arrival (DoA) estimation with Coarray can resolve $O(N^2)$ sources via only $O(N)$ physical sensor elements. When it comes to model errors, i.e., manual coupling, gain and/or phase errors, and sensor location errors, whether Coarray is still effective for degree-of-freedom (DoF) enhancement has not been proved yet. In addition, calibration of the Coarray is also an open problem, which deserves more attentions. This paper formulates the error models of Coarray at first and then proves that the problem of Coarray calibration can be reformulated into an equivalent one of imperfect uniform linear array correction; meanwhile, DoF enhancement is promised. Based on these models, the problem of Coarray calibration, more specifically, joint DoA and error coefficients estimation, can be solved via the existing state-of-the-art array calibration schemes. An excellent scheme named sparse Bayesian array calibration is adopted as an example to estimate DoA and error coefficients jointly in this paper. Simulation results illustrate that for DoA estimation with imperfect Coarray, the calibrated estimator is effective for DoF enhancement and more robust than uncalibrated subspace method.

INDEX TERMS Direction-of-arrival (DoA), model errors, coarray, sparse Bayesian learning (SBL).

I. INTRODUCTION

Direction-of-arrival (DoA) estimation is critical in radar, sonar and wireless communication systems [1], [2]. The state-of-the-art eigenstructure based algorithms can produce super-resolution and accurate estimations, such as MUSIC [3] and ESPRIT [4]. However, the excellent performance of these methods relies on the precise signal model of the data collection system, composed of antennas and radio frequency (RF) chains, and baseband processor. In application of real system, the antennas will interact with each other inevitably due to mutual coupling [5]. Meanwhile, there are usually mismatch between gain and phase of RF chains as well as sensor locations. All those effects mentioned above are referred to as model errors, which will lead to degradation of DoA estimators.

In order to make DoA estimators more robust against the model errors, numerous self-calibrating algorithms have been proposed in the past decades. Wiess *et al.* studied the array correction schemes comprehensively in [6]–[8] corresponding to mutual coupling, gain and/or phase errors, and position mismatch calibration, respectively. The methods proposed in [6]–[8] estimate DoA and unknown parameters jointly by optimizing the objective function over direction and the unknown parameters iteratively. The problem of these algorithms is that the convergence of global minimal is not guaranteed. A maximal likelihood (ML) based position mismatch correction scheme is proposed in [8] which estimates DoA and unknown parameters successively, also, the convergence relies heavily on the initialization. The studies [9]–[14] focus on the calibration of mutual coupling. A closed-form solution of DoA and mutual coupling matrix is derived in [9], which is based on alternating minimization procedure, however, it is only effective for ULA. With the application of sparse Bayesian learning (SBL) in array processing, a great number of joint DoA and mutual coupling coefficients estimation algorithms are proposed under the framework of SBL in recent years [10]–[13]. It has been widely accepted that the SBL based array calibration methods are able to obtain excellent results, especially in the scenario of low signal to noise ratio (SNR) and lack of snapshots. The study [14] estimates

DOA and mutual coupling coefficients for uniform rectangular arrays (URAs) based on banded symmetric Toeplitz matrices.

Coarray is proposed to raise the degree of freedom (DoF) of DoA estimators from $O(N)$ to $O(N^2)$ [15], [16]. Two kinds of well-known Coarray have attracted lots of attention, i.e., nested array [15] and Co-Prime array [16]. Their performances were analyzed in [17] and [18]. The study [19] proposes the algorithm to estimates DoA in the scenario of a mixture of circular and non-circular impinging signals for Coarray. It is unavoidable that Coarrays also suffer from mutual coupling, gain and phase errors, and sensor location errors. The model errors bring challenge for real application of Coarray, thus, the calibration of Coarray deserves more attentions. Current literature focus on the study of mutual coupling and gain and/or phase errors. A scheme of gain and phase errors correction for the nested array is proposed in [20], which employs the partial Toeplitz structure of the covariance matrix and the sparse total least squares (STLS) to calibrate gain and phase errors, respectively. Although many mutual coupling reduction techniques for the nested array exist in the literature [21]–[24], there is little work on mutual coupling calibration for it. The basic idea of mutual coupling reduction array design is to place elements as far from each other as possible to reduce the mutual coupling. A calibration strategy for mutual coupling of the nested circular array was proposed in [25], however, the mutual coupling matrix (MCM) was not acquired during online processing, but by offline simulation via electromagnetic simulation software FEKO. The study [26] performs a detailed performance analysis of Coarray-based MUSIC with sensor location errors, e.g., Cramér-Rao bound (CRB), and mean-squared error (MSE). However, the calibration of location errors for Coarray is still missing in the literature.

Actually, when it comes to model errors, whether the Coarray is still effective in DoF enchantment has not been studied yet. Therefore, before calibrate on, we have to study the model errors of Coarray first. In this paper, we focus on the single type model error, in other word, treat mutual coupling, gain and/or phase errors, and sensor location errors separately. Based on these models, we find that imperfect Coarray can be transformed into a larger virtual ULA with effective mutual coupling, gain and phase errors, or sensor location errors. This finding confirms that Coarray is still effective for DoF enhancement in the presence of model errors. In addition, general model error calibration algorithms proposed in [6]–[8] and [10]–[13] can be utilized to estimate DoA and error coefficients based on these models. In this paper, sparse Bayesian learning array calibration (SBAC) [27] is adopted as an example to solve the problem we formulated.

The rest of this paper is organized as follows. Section II introduces the signal model of Coarray especially for the nested array and the Co-Prime array. Section III studies the signal models of Coarray with mutual coupling, gain and phase errors, and sensor location errors. Section IV describes how to solve our proposed model via SBAC. Section VI and VII show numerical simulation results and conclusion, respectively. The notations used in this paper are introduced as follows: $\odot$, $\otimes$, and $\boxdot$ denote Hadamard product, Kronecker product, and Khatri-Rao product (i.e., the column-wise Kronecker product) of matrices, respectively. $(\cdot)^*$, $(\cdot)^T$, and $(\cdot)^H$ denote conjugate, transpose, and conjugate transpose of matrix, respectively. $\mathbf{X}_{:,i}$, $\mathbf{X}_{i,:}$, and $\mathbf{X}_{i,j}$ denote the ith column, the ith row, and the (i,j)th element of matrix $\mathbf{X}$. $\mathbf{A}_{\mathbb{D}}$ denotes the manifold matrix of an array whose elements locations are given by the set $\mathbb{D}$. diag($\mathbf{c}$) means creating a diagonal matrix with the elements of vector $\mathbf{c}$ on the diagonal. Matrix function vec($\mathbf{X}$) means stacking the columns of $\mathbf{X}$ to form a vector.

II. SIGNAL MODEL OF COARRAY

Consider a nonuniform linear array whose elements are placed on a nonuniform linear grid with d_i being the position of the ith element. Let $\mathbb{D} = \{d_1, d_2, \cdots, d_M\}$ be the elements position set. P uncorrelated narrow band sources impinging upon the array from different directions. The received signals can be written as

$$\mathbf{y}(t) = \mathbf{A}_{\mathbb{D}}\mathbf{x}(t) + \mathbf{n}(t) \tag{1}$$

where $\mathbf{y}(t)$, $\mathbf{x}(t)$, and $\mathbf{n}(t)$ denote the received signal vector, incident signal vector, and noise vector, respectively. The subscript "$\mathbb{D}$" of matrix $\mathbf{A}_{\mathbb{D}}$ means that $\mathbf{A}_{\mathbb{D}}$ is the manifold matrix of the array whose elements locations are given by set $\mathbb{D}$. $(\mathbf{A}_{\mathbb{D}})_{m,p} = e^{j\frac{2\pi}{\lambda}d_m\sin(\theta_p)}$ is the (m,p)th elements of $\mathbf{A}_{\mathbb{D}}$, and λ is carrier wavelength, θ_p is the direction of the pth signal, and M is the number of elements of the array.

Assume that noise is uncorrelated temporally and spatially, the covariance matrix of received signals can be expressed as

$$\mathbf{R}_{\mathbf{yy}} = E[\mathbf{y}(t)\mathbf{y}(t)^H] = \mathbf{A}_{\mathbb{D}}\mathbf{R}_{\mathbf{xx}}\mathbf{A}_{\mathbb{D}}^H + \sigma^2\mathbf{I} \tag{2}$$

where $\mathbf{R}_{\mathbf{xx}}$ is covariance matrix of incident signals. We assume that the incident signals are uncorrelated spatially so that $\mathbf{R}_{\mathbf{xx}}$ is a diagonal matrix. Vectorizing $\mathbf{R}_{\mathbf{yy}}$ as follows

$$\mathbf{z} = \mathrm{vec}(\mathbf{R}_{\mathbf{yy}}) = (\mathbf{A}_{\mathbb{D}}^* \boxdot \mathbf{A}_{\mathbb{D}})\mathbf{p} + \sigma^2\mathbf{1}_n \tag{3}$$

where $\mathbf{p}$ is signal power vector consisting of the diagonal elements of $\mathbf{R}_{\mathbf{xx}}$, and $\mathbf{1}_n$ is formulated by vectorizing of the identical matrix $\mathbf{I}$. $\mathbf{A}_{\mathbb{D}}^* \boxdot \mathbf{A}_{\mathbb{D}}$ behaves like the manifold matrix of a longer array whose sensor locations are given by the values in the set $\mathbb{S} = \{d_m - d_n | m, n = 1, 2, \cdots, M\}$ where d_m denotes the position of the mth sensor of the original array. Let $\mathbf{A}_{\mathbb{S}} = \mathbf{A}_{\mathbb{D}}^* \boxdot \mathbf{A}_{\mathbb{D}}$, (3) can be rewritten as

$$\mathbf{z} = \mathbf{A}_{\mathbb{S}}\mathbf{p} + \sigma^2\mathbf{1}_n. \tag{4}$$

It's unavoidable that various pairs of d_m and d_n result in identical value of difference $d_m - d_n$. The repeated difference leads to a reduction of the cardinality of the set $\mathbb{S}$, assuming that the redundant elements have been removed from $\mathbb{S}$. As long as the elements locations set of the original array $\mathbb{D}$ are designed specifically, the cardinality of set $\mathbb{S}$ will be much larger than $\mathbb{D}$, in other words, a larger virtual array is produced. Thus, performing DoA estimation via the model (4) will obtain higher DoF. Two typical kinds of such arrays are the nested and Co-Prime arrays, which are defined as follows.

Definition 1 (Nested Array): The K level nested array is defined as one where the elements locations are given by the set $\mathbb{D}^{NA}$ as

$$\begin{aligned}\mathbb{D}^{NA} &= \bigcup_{k=1}^{K} \mathbb{D}_k^{NA} \\ \mathbb{D}_1^{NA} &= \{m\Delta d, m = 1, 2, \cdots, N_1\} \\ \mathbb{D}_k^{NA} &= \{m\Delta d \cdot \prod_{i=1}^{k-1}(N_i + 1), m = 1, 2, \cdots, N_k\}, \\ &\qquad k = 2, 3, \cdots, K \end{aligned} \tag{5}$$

where K is the number of levels, and Δd is minimum inter-element spacing usually chosen as $\Delta d = \lambda/2$.

Definition 2 (Co-Prime Array): The Co-Prime array is defined as one where the elements locations are given by the set $\mathbb{D}^{CoA}$ as

$$\mathbb{D}^{CoA} = \{Mn \cdot \Delta d, 0 \le n \le N-1\} \bigcup \{Nm \cdot \Delta d, 0 \le m \le 2M-1\} \tag{6}$$

with $M < N$ being prime integers.

If the locations set of the original array is given by $\mathbb{D}^{NA}$, the cardinality of $\mathbb{S}$ can reach $O(N^2)$ with $N = N_1 + N_2 + \cdots + N_K$. In other words, the DoF of the nested array can be raised to $O(N^2)$ with only $O(N)$ physical elements. Similarly, the DoF of the Co-Prime array will reach $O(MN)$ with only $O(M+N)$ physical elements.

III. ERROR MODELS OF COARRAY

A. MUTUAL COUPLING OF THE NESTED ARRAY

The mutual coupling describes the electromagnetic interactions of array elements. The placement of the sensors for Coarray is not uniform any more. As a result, the mutual coupling matrix of this kind of array is not a Toeplitz matrix, but depends on the individual array structure instead. This subsection focuses on the mutual coupling of the nested array. From the **Definition 1** we can find that the structure of the nested array can be viewed as the placement of K different ULAs (with different inter-element spacing) head-to-tail in a line. The inter-element spacing of the first subarray is Δd, but is $\Delta d \cdot \prod_{i=1}^{k-1}(N_i+1)$ for the kth subarray. The effect of mutual coupling decreases dramatically with the increase of distance. Therefore, it is reasonable to just consider the mutual coupling of the first subarray. With the effect of mutual coupling, the array output can be represented as

$$\mathbf{y}(t) = \mathbf{C}\mathbf{A}_{\mathbb{D}}\mathbf{x}(t) + \mathbf{n}(t) \tag{7}$$

where

$$\mathbf{C} = \begin{bmatrix} \mathbf{B}_{N_1\times N_1} & \mathbf{0}_{N_1\times(N-N_1)} \\ \mathbf{0}_{(N-N_1)\times N_1} & \mathbf{I}_{(N-N_1)\times(N-N_1)} \end{bmatrix} \tag{8}$$

is referred to as the MCM. Matrix $\mathbf{B}_{N_1\times N_1} = \text{Teoplitz}(1, c_1, c_2, \cdots, c_{N_1-1})$ represents the MCM of the first subarray, and the rest mutual coupling coefficients are set to zeros. $\mathbf{0}_{M\times N}$ is $M \times N$ all-zero matrix with all elements are zeros, $\mathbf{I}_{M\times M}$ is the identical matrix. The covariance matrix of received signals is

$$\mathbf{R_{yy}} = \mathbf{C}\mathbf{A}_{\mathbb{D}}\mathbf{R_{xx}}\mathbf{A}_{\mathbb{D}}^H\mathbf{C}^H + \sigma^2\mathbf{I}. \tag{9}$$

Vectorizing (9), we get

$$\mathbf{z} = \text{vec}(\mathbf{R_{yy}}) = [(\mathbf{C}\mathbf{A}_{\mathbb{D}})^* \boxdot (\mathbf{C}\mathbf{A}_{\mathbb{D}})] \cdot \mathbf{p} + \sigma^2\mathbf{1_n}. \tag{10}$$

The model (10) denotes the signal model of the nested array, where $\mathbf{z}$ is equivalent to received signal, and $(\mathbf{C}\mathbf{A}_{\mathbb{D}})^* \boxdot (\mathbf{C}\mathbf{A}_{\mathbb{D}})$ plays the role of array manifold matrix with the effect of mutual coupling. One can check whether $(\mathbf{C}\mathbf{A}_{\mathbb{D}})^* \boxdot (\mathbf{C}\mathbf{A}_{\mathbb{D}})$ can be constructed based on the virtual elements locations set $\mathbb{S}$ or not. If the answer is yes, we can confirm that the Coarray in the presence of mutual coupling can be transformed into an imperfect ULA, therefore, it can be used for DoF enhancement. This assumption can be expressed by the following relationship

$$(\mathbf{C}\mathbf{A}_{\mathbb{D}})^* \boxdot (\mathbf{C}\mathbf{A}_{\mathbb{D}}) = \mathbf{C}'\mathbf{A}_{\mathbb{S}} \tag{11}$$

where $\mathbf{C}'$ behaves like the equal mutual coupling matrix and can be represented analytically by $\mathbf{C}$. $\mathbf{A}_{\mathbb{S}} = \mathbf{A}_{\mathbb{D}}^* \boxdot \mathbf{A}_{\mathbb{D}}$ is equivalent to the manifold matrix of virtual array without model errors. The relationship of (11) can be described and proved by **Theorem 1** (see Appendix A) [28].

It follows from **Theorem 1** that the equivalent mutual coupling matrix can be constructed as

$$\mathbf{C}' = \begin{bmatrix} \mathbf{B}'_{N_1N\times N_1N} & \mathbf{0}_{N_1N\times(N^2-N_1N)} \\ \mathbf{0}_{(N^2-N_1N)\times N_1N} & \bar{\mathbf{C}}_{(N^2-N_1N)\times(N^2-N_1N)} \end{bmatrix}_{N_1^2\times N_1^2} \tag{12}$$

where

$$\mathbf{B}'_{N_1N\times N_1N} = \mathbf{B}^*_{N_1\times N_1} \otimes \mathbf{C}_{N\times N} \tag{13a}$$
$$\bar{\mathbf{C}}_{(N^2-N_1N)\times(N^2-N_1N)} = \mathbf{I}_{(N-N_1)\times(N-N_1)} \otimes \mathbf{C}_{N\times N} \tag{13b}$$

The effect of mutual coupling is contained in matrix $\mathbf{B}'_{N_1N\times N_1N}$, where N_1 and N are the number of elements of the first subarray and total array, respectively.

As a result, (10) can be simplified into

$$\mathbf{z} = \mathbf{C}'\mathbf{A}_{\mathbb{S}}\mathbf{p} + \sigma^2\mathbf{1_n} \tag{14}$$

where $\mathbf{C}'$ and $\mathbf{A}_{\mathbb{S}}$ are MCM and steering matrix of virtual array, specifically, a longer ULA, respectively. The effect mutual coupling matrix $\mathbf{C}'$ can be represented analytically by $\mathbf{C}$. Therefore, numerous state-of-the-art mutual coupling calibration algorithms can be applied to estimate $\mathbf{C}'$ and $\mathbf{p}$ based on the model (14).

B. GAIN AND/OR PHASE ERRORS

Suppose that the gain errors vector of the sensors is $\boldsymbol{\eta} = [\eta_1, \eta_2, \cdots, \eta_M]^T$, and the phase disturbance vector is $\boldsymbol{\phi} = [\exp(j\phi_1), \exp(j\phi_2), \cdots, \exp(j\phi_M)]^T$. The array output with gain and phase errors is

$$\mathbf{y}(t) = (\mathbf{I} + \boldsymbol{\Psi}\boldsymbol{\Phi})\mathbf{A}_{\mathbb{D}}\mathbf{x}(t) + \mathbf{n}(t) \tag{15}$$

where $\mathbf{\Phi}$ and $\mathbf{\Psi}$ represent phase and gain errors matrices with $\mathbf{\Phi} = \mathrm{diag}(\exp(j\phi_1), \exp(j\phi_2), \cdots, \exp(j\phi_M))$ and $\mathbf{\Psi} = \mathrm{diag}(\eta_1, \eta_2, \cdots, \eta_M)$, respectively. For notational simplification, let $\mathbf{\Xi} = \mathbf{I} + \mathbf{\Psi}\mathbf{\Phi}$ and (15) can be written as

$$\mathbf{y}(t) = \mathbf{\Xi}\mathbf{A}_{\mathbb{D}}\mathbf{x}(t) + \mathbf{n}(t). \tag{16}$$

Calculating the covariance matrix of received signal and performing vectorizing, we get

$$\mathbf{z} = [(\mathbf{\Xi}\mathbf{A}_{\mathbb{D}})^* \boxdot (\mathbf{\Xi}\mathbf{A}_{\mathbb{D}})] \cdot \mathbf{p} + \sigma^2\mathbf{1}_{\mathbf{n}}. \tag{17}$$

Similar to the mutual coupling case, the model (17) is expected to be reformulated as

$$\mathbf{z} = \mathbf{\Xi}'\mathbf{A}_{\mathbb{S}}\mathbf{p} + \sigma^2\mathbf{1}_{\mathbf{n}} \tag{18}$$

where $\mathbf{\Xi}'$ behaves like the gain and phase errors matrix of the virtual array, which can be represented analytically by $\mathbf{\Xi}$. **Lemma 1** provides the support of the transformation from (17) to (18).

Lemma 1: For $M \times M$ diagonal matrix $\mathbf{C} = \mathrm{diag}(c_1, c_2, \cdots, c_M)$ and $M \times P$ matrix $\mathbf{A}$, the following relationship holds:

$$(\mathbf{CA})^* \boxdot (\mathbf{CA}) = \mathbf{C}'\mathbf{A}' \tag{19}$$

where

$$\mathbf{C}' = \mathrm{diag}(\mathbf{c}_1, \mathbf{c}_2, \cdots, \mathbf{c}_M) \tag{20a}$$
$$\mathbf{c}_i = [c_i^* c_1, c_i^* c_2, \cdots, c_i^* c_M] \tag{20b}$$
$$\mathbf{A}' = \mathbf{A}^* \boxdot \mathbf{A} \tag{20c}$$

Proof: It follows from Theorem 1 that

$$(\mathbf{CA})^* \boxdot (\mathbf{CA}) = \mathbf{C}' \cdot (\mathbf{A}^* \boxdot \mathbf{A}) \tag{21}$$

Matrix $\mathbf{C}'$ has the block form

$$\mathbf{C}' = \begin{bmatrix} [\mathbf{C}]_{1,1} & [\mathbf{C}]_{1,2} & \cdots & [\mathbf{C}]_{1,M} \\ [\mathbf{C}]_{2,1} & [\mathbf{C}]_{2,2} & \cdots & [\mathbf{C}]_{2,M} \\ & & \vdots & \\ [\mathbf{C}]_{M,1} & [\mathbf{C}]_{M,2} & \cdots & [\mathbf{C}]_{M,M} \end{bmatrix} \tag{22}$$

where

$$[\mathbf{C}]_{m,n} = c_{m,n}^*\mathbf{C} \tag{23}$$

is the (m, n)th block of $\mathbf{C}'$. In this case, $\mathbf{C}$ denotes the gain and phase errors of original array (Coarray), and is a diagonal matrix, therefore,

$$c_{m,n} = \begin{cases} c_m & m = n \\ 0 & m \neq n \end{cases} \tag{24}$$

As a result,

$$\mathbf{C}' = \begin{bmatrix} [\mathbf{C}]_{1,1} & & & \\ & [\mathbf{C}]_{2,2} & & \\ & & \ddots & \\ & & & [\mathbf{C}]_{M,M} \end{bmatrix} \tag{25}$$

is a blocking diagonal matrix. Actually, each block of $\mathbf{C}'$ is diagonal, therefore, $\mathbf{C}'$ is a diagonal matrix as well

$$\mathbf{C}' = \mathrm{diag}(c_1^*\mathbf{c}, c_2^*\mathbf{c}, \cdots, c_M^*\mathbf{c}). \tag{26}$$

□

It follows from **Lemma 1** that the matrix $\mathbf{\Xi}'$ can be constructed via $\mathbf{\Xi}$. Therefore, the unknown matrix $\mathbf{\Xi}'$ and vector $\mathbf{p}$ in the model (18) can be estimated using exist methods, such as the schemes proposed in [7] and [27].

C. SENSOR LOCATION ERRORS

Suppose that the true position vector of the array is $\mathbf{d} = [d_1, d_2, \cdots, d_M]^T$, the position perturbation vector is $\Delta\mathbf{d} = [\Delta d_1, \Delta d_2, \cdots, \Delta d_M]^T$. The manifold matrix of the array with sensor location errors is

$$\tilde{\mathbf{A}}_{\mathbb{D}} = \begin{bmatrix} e^{j2\pi/\lambda(d_1+\Delta d_1)\sin(\theta_1)} & \ldots & e^{j2\pi/\lambda(d_1+\Delta d_1)\sin(\theta_P)} \\ e^{j2\pi/\lambda(d_2+\Delta d_2)\sin(\theta_1)} & \ldots & e^{j2\pi/\lambda(d_2+\Delta d_2)\sin(\theta_P)} \\ & \vdots & \\ e^{j2\pi/\lambda(d_M+\Delta d_M)\sin(\theta_1)} & \ldots & e^{j2\pi/\lambda(d_M+\Delta d_M)\sin(\theta_P)} \end{bmatrix}. \tag{27}$$

Let $\mathbf{A}_{\mathbb{D}}$ and $\mathbf{A}_{\Delta\mathbb{D}}$ represent true array manifold matrix and perturbation matrix, respectively. The matrix $\tilde{\mathbf{A}}_{\mathbb{D}}$ can be written as

$$\tilde{\mathbf{A}}_{\mathbb{D}} = \mathbf{A}_{\mathbb{D}} \odot \mathbf{A}_{\Delta\mathbb{D}} \tag{28}$$

where

$$(\mathbf{A}_{\mathbb{D}})_{m,p} = e^{j2\pi/\lambda d_m \sin(\theta_p)} \tag{29a}$$
$$(\mathbf{A}_{\Delta\mathbb{D}})_{m,p} = e^{j2\pi/\lambda \Delta d_m \sin(\theta_p)} \tag{29b}$$
$$1 \leq m \leq M, \quad 1 \leq p \leq P. \tag{29c}$$

The received signals of the array in the presence of sensor location errors are

$$\mathbf{y}(t) = (\mathbf{A}_{\mathbb{D}} \odot \mathbf{A}_{\Delta\mathbb{D}})\mathbf{s}(t) + \mathbf{n}(t). \tag{30}$$

By calculating the covariance matrix of received signal and performing vectorizing, we have

$$\mathbf{z} = \left[(\mathbf{A}_{\mathbb{D}} \odot \mathbf{A}_{\Delta\mathbb{D}})^* \boxdot (\mathbf{A}_{\mathbb{D}} \odot \mathbf{A}_{\Delta\mathbb{D}})\right] \cdot \mathbf{p} + \sigma^2\mathbf{1}_{\mathbf{n}}. \tag{31}$$

The model (31) is expected to be reformulated as

$$\mathbf{z} = (\mathbf{A}_{\Delta\mathbb{S}} \odot \mathbf{A}_{\mathbb{S}})\mathbf{p} + \sigma^2\mathbf{1}_{\mathbf{n}} \tag{32}$$

with $\mathbf{A}_{\mathbb{S}} = \mathbf{A}_{\mathbb{D}}^* \boxdot \mathbf{A}_{\mathbb{D}}$ and $\mathbf{A}_{\Delta\mathbb{S}} = \mathbf{A}_{\Delta\mathbb{D}}^* \boxdot \mathbf{A}_{\Delta\mathbb{D}}$. The model (32) can be viewed as an imperfect ULA which can be calibrated by further step. Actually, (32) shows that a Coarray with locations errors shares the similar signal model with an imperfect ULA. **Lemma 2** provides the support of the transformation from (31) to (32).

Lemma 2: For $M \times P$ matrix $\mathbf{C}$ and $M \times P$ matrix $\mathbf{A}$, the following relationship can be established:

$$(\mathbf{C} \odot \mathbf{A})^* \boxdot (\mathbf{C} \odot \mathbf{A}) = \mathbf{C}' \odot \mathbf{A}' \tag{33}$$

where

$$\mathbf{C}' = \mathbf{C}^* \boxdot \mathbf{C} \tag{34a}$$
$$\mathbf{A}' = \mathbf{A}^* \boxdot \mathbf{A}. \tag{34b}$$

Proof: Let $\mathbf{B} = (\mathbf{C} \odot \mathbf{A})^* \boxdot (\mathbf{C} \odot \mathbf{A})$, from the definition of Khatri-Rao product, we can get

$$\mathbf{B}_{:,p} = (\mathbf{C} \odot \mathbf{A})_{:,p}^* \otimes (\mathbf{C} \odot \mathbf{A})_{:,p} \tag{35a}$$
$$= (\mathbf{C}_{:,p} \odot \mathbf{A}_{:,p})^* \otimes (\mathbf{C}_{:,p} \odot \mathbf{A}_{:,p}). \tag{35b}$$

It follows from the definition of Hadamard and Kronecker product, $\mathbf{B}_{:,p}$ can be written as follows

$$\mathbf{B}_{:,p} = \begin{pmatrix} c_{1,p}^* a_{1,p}^* \mathbf{C}_{:,p} \odot \mathbf{A}_{:,p} \\ \vdots \\ c_{m,p}^* a_{m,p}^* \mathbf{C}_{:,p} \odot \mathbf{A}_{:,p} \\ \vdots \\ c_{M,p}^* a_{M,p}^* \mathbf{C}_{:,p} \odot \mathbf{A}_{:,p} \end{pmatrix} \begin{matrix} \\ \\ \leftarrow \text{The } m\text{th Block} \\ \\ \\ \end{matrix} \tag{36a}$$

$$= \begin{pmatrix} c_{1,p}^* \mathbf{c}_p \odot a_{1,p}^* \mathbf{a}_p \\ \vdots \\ c_{m,p}^* \mathbf{c}_p \odot a_{m,p}^* \mathbf{a}_p \\ \vdots \\ c_{M,p}^* \mathbf{c}_p \odot a_{M,p}^* \mathbf{a}_p \end{pmatrix} \begin{matrix} \\ \\ \leftarrow \text{The } m\text{th Block} \\ \\ \\ \end{matrix} \tag{36b}$$

$$= (\mathbf{c}_p^* \otimes \mathbf{c}_p) \odot (\mathbf{a}_p^* \otimes \mathbf{a}_p) \tag{36c}$$

where

$$\mathbf{c}_p = \mathbf{C}_{:,p} = [c_{1,p}, c_{2,p}, \cdots, c_{M,p}]^T \tag{37a}$$

$$\mathbf{a}_p = \mathbf{A}_{:,p} = [a_{1,p}, a_{2,p}, \cdots, a_{M,p}]^T. \tag{37b}$$

Based on (36), the matrix $\mathbf{B} = [\mathbf{B}_{:,1}, \mathbf{B}_{:,2}, \cdots, \mathbf{B}_{:,P}]$ can be reconstructed as

$$\begin{aligned} \mathbf{B} &= [(\mathbf{c}_1^* \otimes \mathbf{c}_1) \odot (\mathbf{a}_1^* \otimes \mathbf{a}_1), \cdots, (\mathbf{c}_P^* \otimes \mathbf{c}_P) \odot (\mathbf{a}_P^* \otimes \mathbf{a}_P)] \\ &= [(\mathbf{c}_1^* \otimes \mathbf{c}_1), \cdots, (\mathbf{c}_P^* \otimes \mathbf{c}_P)] \odot [(\mathbf{a}_1^* \otimes \mathbf{a}_1), \cdots, \\ &\quad (\mathbf{a}_P^* \otimes \mathbf{a}_P)]. \end{aligned} \tag{38a}$$

Obviously, we can get

$$\mathbf{B} = (\mathbf{C}^* \boxdot \mathbf{C}) \odot (\mathbf{A}^* \boxdot \mathbf{A}). \tag{39}$$

□

Following as the instruction of **Lemma 2**, matrix $\mathbf{A}_{\Delta\mathbb{S}}$ can be represented analytically, with

$$(\mathbf{A}_{\Delta\mathbb{S}})_{(m-1)M+n,p} = e^{j2\pi/\lambda \Delta d_{m,n} \sin(\theta_p)} \tag{40}$$

being the $((m-1)M+n, p)$th element. $\Delta d_{m,n} = \Delta d_m - \Delta d_n$ is the difference of the mth and nth elements in $\Delta\mathbb{D}$. In addition, it is also the $((m-1)M+n)$th element of set $\Delta\mathbb{S}$. Actually, $\Delta d_{m,n}$ is tiny compared to the carrier wavelength, and an approximation can be obtained according to the first-order Taylor expansion that $e^{j2\pi/\lambda \Delta d_{m,n} \sin(\theta_p)} \approx 1 + j2\pi/\lambda \Delta d_{m,n} \sin(\theta_p)$. As a result, $\mathbf{A}_{\Delta\mathbb{S}}$ can be approximated by

$$\mathbf{A}_{\Delta\mathbb{S}} = \begin{bmatrix} 1 + j2\pi/\lambda \Delta d_1 \sin(\theta_1) \cdots 1 + j2\pi/\lambda \Delta d_1 \sin(\theta_P) \\ 1 + j2\pi/\lambda \Delta d_2 \sin(\theta_1) \cdots 1 + j2\pi/\lambda \Delta d_2 \sin(\theta_P) \\ \vdots \\ 1 + j2\pi/\lambda \Delta d_M \sin(\theta_1) \cdots 1 + j2\pi/\lambda \Delta d_M \sin(\theta_P) \end{bmatrix}. \tag{41}$$

The change of $\mathbf{A}_{\Delta\mathbb{S}}$ not only depends on the position perturbation Δd_m but also on the induced signal direction θ_p. Fortunately, that the row of $\mathbf{A}_{\Delta\mathbb{S}}$ is only related to Δd_m, and each column is only related to the individual induced signal direction θ_p. With the approximation of $\mathbf{A}_{\Delta\mathbb{S}}$, (32) can be rewritten as

$$\mathbf{z} = \mathbf{A}_{\mathbb{S}}\mathbf{p} + (\mathbf{A}_{\mathbb{S}} \odot \mathbf{A}'_{\Delta\mathbb{S}})\mathbf{p} + \sigma^2 \mathbf{1_n} \tag{42}$$

where, $\mathbf{A}'_{\Delta\mathbb{S}} = \mathbf{A}_{\Delta\mathbb{S}} - \Pi$ with Π being the matrix where all elements are 1. The first term of the right hand side of (42) denotes the non-disturbed component, and the second term describes the disturbed component related to the position mismatch. Considering the special structure of $\mathbf{A}'_{\Delta\mathbb{S}}$, the impact of the disturbed component in (42) can be expressed separately by two diagonal matrix $\mathbf{D}$ and $\mathbf{\Theta}$, therefore,

$$\mathbf{z} = \mathbf{A}_{\mathbb{S}}\mathbf{p} + (\mathbf{D}\mathbf{A}_{\mathbb{S}}\mathbf{\Theta})\mathbf{p} + \sigma^2 \mathbf{1_n} \tag{43}$$

where

$$\mathbf{D} = \mathrm{diag}(\Delta d_{1,1}, \Delta d_{1,2}, \cdots, \Delta d_{M,M}) \tag{44a}$$

$$\mathbf{\Theta} = \mathrm{diag}(j2\pi/\lambda \sin(\theta_1), j2\pi/\lambda \sin(\theta_2), \cdots, j2\pi/\lambda \sin(\theta_P)). \tag{44b}$$

The unknown matrix $\mathbf{D}$ and vector $\mathbf{p}$ in model (44) can be estimated easily using the methods proposed in [8] and [27].

IV. MODEL ERROR CORRECTION VIA SBAC

So far, models of Coarray with unknown errors, (i.e., the mutual coupling, gain and/or phase errors, and sensor location errors) have been established and studied in Section III. It has been proved that Coarray, such as the nested array and Co-Prime array, with single type of model error still can be utilized to estimate DoA with higher DoF as long as proper calibration is performed. Actually, the signal model of Coarray with model errors has the same form as imperfect ULA. Therefore, numerous state-of-the-art on-line array calibration algorithms can be utilized to estimate the unknown error coefficients and DoA based on these models.

Weiss *et al.* have studied the problem of array correction and proposed three estimators of DoA and error parameters in [6]–[8] corresponding to three different kinds of model errors. An unified framework of array calibration based on SBL has been proposed in [27], which is called SBAC. It can correct all three kinds of model errors mentioned in this paper, therefore, is adopted to solve the problems proposed in Section III. This section introduces the joint DoA and unknown error coefficients estimation via SBAC based on the models formulated in Section III.

The model (14) (18) (44) can be written into the form of free-disturb component plus disturb component [27]

$$\mathbf{z} = \mathbf{A}\mathbf{p} + \mathbf{Q}\boldsymbol{\upsilon} + \sigma^2 \mathbf{1_n} \tag{45}$$

where the first term of the right hand side of (45) represents disturbance-free component, and the second term denotes disturbance component caused by model error $\mathbf{Q}\boldsymbol{\upsilon} = (\mathbf{A}' - \mathbf{A})\mathbf{p}$. All three kinds of error models can be described by the model (45), the only difference of three error models is the construction of $\boldsymbol{\upsilon}$ and $\mathbf{Q}$.

1) Mutual coupling

$$\boldsymbol{\upsilon} = \mathbf{c}^* \otimes \mathbf{c} \tag{46a}$$

$$\mathbf{Q}_{:,p} = \mathbf{G}_p \Phi(\theta)\mathbf{p} \tag{46b}$$
$$\mathbf{G}_p = \partial \mathbf{C}'/\partial \boldsymbol{\upsilon}_p \tag{46c}$$

where $\Phi(\theta) = \mathbf{A}(\theta)$. Matrix $\mathbf{C}'$ is constructed using (12), vector $\mathbf{c}$ is the mutual coupling coefficients of the original array (Coarray), and $\boldsymbol{\upsilon}$ is equivalent coefficients for expanded array (ULA) whose elements locations are given by $\mathbb{S}$.

2) Gain and/or phase errors

$$\boldsymbol{\upsilon} = \boldsymbol{\kappa}^* \otimes \boldsymbol{\kappa} \tag{47a}$$
$$\mathbf{Q}_{:,p} = \mathbf{G}_p \Phi(\theta)\mathbf{p} \tag{47b}$$
$$\mathbf{G}_p = \partial(\mathrm{diag}(\boldsymbol{\upsilon}))/\partial \boldsymbol{\upsilon}_p \tag{47c}$$

where $\Phi(\theta) = \mathbf{A}(\theta)$. Vector $\boldsymbol{\kappa}$ plays a comprehensive role in the effect of gain and phase errors with $\kappa_m = \eta_m \cdot \phi_m - 1$, and $\boldsymbol{\upsilon}$ is the equivalent gain and phase errors coefficients vector of expanded ULA.

3) Locations errors

$$\boldsymbol{\upsilon} = \Delta\mathbf{d} \ominus \Delta\mathbf{d} \tag{48a}$$
$$\mathbf{Q}_{:,p} = \mathbf{G}_p \Phi(\theta)\mathbf{p} \tag{48b}$$
$$\mathbf{G}_p = \partial(\mathrm{diag}(\boldsymbol{\upsilon}))/\partial \boldsymbol{\upsilon}_p \tag{48c}$$

where $\Phi(\theta) = \mathbf{A}(\theta)\boldsymbol{\Theta}(\theta)$. Vector $\Delta\mathbf{d}$ is the position error vector, $\ominus$ is an operator similar to the Kronecker product which replaces the multiplication by minus. $\boldsymbol{\upsilon}$ is the equivalent elements locations errors of expanded ULA, and Θ is the direction related error matrix caused by position mismatch.

In the model (45), parameters $\mathbf{p}$, $\boldsymbol{\upsilon}$, and σ^2 can be estimated jointly under the framework of SBL. In order to implement SBL, (45) should be expanded to over-complete form by sampling the potential space into discretely set $\boldsymbol{\Omega} = [\theta_1, \theta_2, \cdots, \theta_N]$. In addition, the signal power vector $\mathbf{p}$ should be zeros-padded to the length of N, which describes the power of candidate signals from the set Ω. The non-zeros elements indexes of vector $\mathbf{p}$ indicate the directions of incident signals. Suppose that noise is zero-mean Gaussian distribution with σ^2 being the variance, and the sparse vector $\mathbf{p}$ is also a zeros-mean Gaussian vector

$$\mathbf{p} \sim \mathcal{N}(\mathbf{0}, \Gamma) \tag{49}$$

where $\Gamma = \mathrm{diag}(\gamma_1, \gamma_2, \cdots, \gamma_N)$ with γ_n being the hyper-parameter of the variance of p_n. The likelihood function is

$$\begin{aligned} p(\mathbf{z}|\mathbf{p}; \boldsymbol{\upsilon}, \sigma^2, \boldsymbol{\gamma}) &= |\pi\sigma^2\mathbf{I}|^{-1} \exp\left(-\sigma^{-2}||\mathbf{z} - \mathbf{A}\mathbf{p} - \mathbf{Q}\boldsymbol{\upsilon}||^2\right) && (50a)\\ &= |\pi\sigma^2\mathbf{I}|^{-1} \exp\left(-\sigma^{-2}||\mathbf{z} - \mathbf{A}'\mathbf{p}||^2\right). && (50b)\end{aligned}$$

The probability density of $\mathbf{z}$ with respect to the unknown parameters is

$$\begin{aligned} p(\mathbf{z}; \boldsymbol{\upsilon}, \sigma^2, \boldsymbol{\gamma}) &= \int p(\mathbf{z}|\mathbf{p}; \boldsymbol{\upsilon}, \sigma^2) \times p(\mathbf{p}; \boldsymbol{\gamma}) d\mathbf{p} && (51a)\\ &= |\pi\Sigma_z|^{-1} \exp\left(-\mathrm{tr}\left(\Sigma_z^{-1}\mathbf{R}_\mathbf{p}\right)\right) && (51b)\end{aligned}$$

where $\Sigma_z = \sigma^2\mathbf{I} + \mathbf{A}'\Gamma(\mathbf{A}')^H$, $\mathbf{R}_\mathbf{p} = \mathbf{p}\mathbf{p}^H$. The estimation of $\boldsymbol{\gamma}$, $\boldsymbol{\upsilon}$, σ^2 can be obtained by maximizing (51) via the EM algorithm. The detailed iteration strategies of parameters $\boldsymbol{\gamma}$, $\boldsymbol{\upsilon}$, and σ^2 are shown in Appendix B, and the implementation of SBAC is summarized in Algorithm 1

Algorithm 1 Coarray Calibration via SBAC

Input: $\mathbf{z}$, $\mathbf{A}$
Output: $\mathbf{p}$, $\boldsymbol{\upsilon}$, σ^2
Initialization: $\boldsymbol{\mu} = \mathbf{A}^H(\mathbf{A}\mathbf{A}^H)^{-1}\mathbf{z}$, $\sigma^2 = ||\mathbf{z}||_2/M^2$, $\boldsymbol{\gamma}_i = ||\boldsymbol{\mu}_{i,:}||_2$
$\mathbf{C} = \mathrm{Toeplitz}[1, 0, \cdots, 0]$ for mutual coupling;
$\mathbf{C} = \mathrm{diag}[1, 1, \cdots, 1]$ for gain and phase errors;
$\mathbf{D} = \mathrm{diag}[0, 0, \cdots, 0]$ for position error;
Define: maxIteration, errorThreshold;
while $n <$ maxIteration or *error* $>$ errorThreshold; **do**
  Updating $\boldsymbol{\upsilon}^{(n)}$ via (68a), (69a) and (70)
  where $\mathbf{Q}$ is calculating via (46b) for mutual coupling;
    $\mathbf{Q}$ is calculating via (47b) for gain and phase errors;
    $\mathbf{Q}$ is calculating via (48b) for position error;
  Reconstruct of $\mathbf{A}'$ with
    $\mathbf{A}' = \mathbf{C}'(\boldsymbol{\upsilon}^{(n)}) \cdot \mathbf{A}$ for mutual coupling, $\mathbf{C}'(\boldsymbol{\upsilon}^{(n)})$ is constructed via (12);
    $\mathbf{A}' = \mathrm{diag}(\boldsymbol{\upsilon}^{(n)}) \cdot \mathbf{A}$ for gain and phase errors;
    $\mathbf{A}' = \mathrm{diag}(\boldsymbol{\upsilon}^{(n)}) \cdot \mathbf{A} \cdot \boldsymbol{\Theta} + \mathbf{A}$ for position error;
  Updating $(\sigma^2)^{(n)}$ via (68b), (69b) and (70);
  Updating $\boldsymbol{\gamma}^{(n)}$ via (68c), (69c) and (70);
  $error = ||\boldsymbol{\gamma}^{(n-1)} - \boldsymbol{\gamma}^{(n)}||_2/||\boldsymbol{\gamma}^{(n-1)}||_2$;
  $n = n + 1$;

The parameters $\boldsymbol{\gamma}$, $\boldsymbol{\upsilon}$, and σ^2 can be obtained after the convergence of iteration described in Algorithm 1. Searching the peaks of the sparse vector $\mathbf{p}$ will obtain the estimates of DoAs.

The equivalent mutual coupling coefficients are formed by $\boldsymbol{\upsilon} = \mathbf{c}^* \otimes \mathbf{c}$, the first element is corrected in general application, therefore, $c_1 = 1$. The rest of the mutual coupling coefficients can be obtained via

$$\bar{\mathbf{c}}_m = [\boldsymbol{\upsilon}]_m./[\boldsymbol{\upsilon}]_1 \tag{52}$$

where $[\boldsymbol{\upsilon}]_m = c_m * \mathbf{c}$ denotes the mth block of $\boldsymbol{\upsilon}$, and $[./]$ is an operator that performing element-by-element divider between two vectors. Vector $\bar{\mathbf{c}}_m$ is the estimate vector of the mth mutual coupling coefficient, which contains several estimates of $\bar{c}_m$. We adopt the mean value of these elements as the estimates of the mth coefficient

$$\bar{c}_m = \mathrm{mean}(\bar{\mathbf{c}}_m) \tag{53}$$

where $\mathrm{mean}(\cdot)$ denotes taking mean value of a vector. The original mutual coupling coefficients can be recovered via (52) and (53), the estimates of gain and phase error can be obtained in the same way.

However, the equivalent locations errors are formed by $\boldsymbol{\upsilon} = \Delta\mathbf{d} \ominus \Delta\mathbf{d}$, which can be written into matrix form

$$\boldsymbol{\Lambda} \cdot \Delta\mathbf{d} = \boldsymbol{\upsilon} \tag{54}$$

where

$$\mathbf{\Lambda} = \begin{pmatrix} [\mathbf{\Lambda}]_1 \\ \vdots \\ [\mathbf{\Lambda}]_m \\ \vdots \\ [\mathbf{\Lambda}]_M \end{pmatrix} \leftarrow \text{The } m\text{th Block.} \quad (55)$$

$[\mathbf{\Lambda}]_m$ is a $M \times M$ matrix where the mth column is all 1 and the rest of columns contain only one nonzero element -1.

$$[\mathbf{\Lambda}]_m = \begin{pmatrix} 0 & \cdots & 0 & 1 & -1 & \cdots & 0 & 0 \\ 0 & \cdots & 0 & 1 & 0 & -1 & \cdots & 0 \\ \vdots & & \vdots & \vdots & \vdots & & \vdots & \vdots \\ 0 & \cdots & 0 & 1 & 0 & \cdots & 0 & -1 \\ \vdots & & \vdots & \vdots & \vdots & & \vdots & \vdots \\ 0 & \cdots & -1 & 1 & 0 & \cdots & 0 & 0 \end{pmatrix}. \quad (56)$$

This is an over determined linear equations, and we can get the estimates of $\Delta\mathbf{d}$ via the least square (LS) method. As a result, the position disturbance can be obtained by

$$\Delta\mathbf{d} = (\mathbf{\Lambda}\mathbf{\Lambda}^H)^{-1}\mathbf{\Lambda}^H \boldsymbol{\upsilon}. \quad (57)$$

So far, both DoA and error coefficients are obtained.

V. THE CRAMÉR-RAO BOUND

In this section, we derive the Cramér-Rao bound (CRB), the lower bound of the minimum variance of an unbiased estimator, for the Coarray in the presence of model errors. The model errors are assumed to be unknown but deterministic parameters. The unknown parameters are DoAs, source powers, noise powers, and model error parameters, i.e., the mutual coupling efficients, the gain errors, the phase errors, and sensor location errors. Assume that the sources are spatially and temporally uncorrelated, meanwhile, the additive noise is spatially and temporally uncorrelated white Gaussian and uncorrelated with the sources. With these assumptions, the fisher information matrix (FIM) can be expressed as [17]:

$$\mathbf{J} = N\mathbf{M}^H(\mathbf{R}^T \otimes \mathbf{R})^{-1}\mathbf{M}. \quad (58)$$

The study [26] provides the CRB of DoAs estimations when in the presence of sensor location errors. In this section, we develop the CRB of DoAs estimates in the presence of mutual coupling and gain and phase error. Denote the DoAs, source powers, noise powers, and the model error coefficients are denoted by $\boldsymbol{\theta}, \boldsymbol{p}, \sigma^2$, and $\boldsymbol{\upsilon}$, respectively. The matrix $\mathbf{M}$ can be expressed as [26]:

$$\mathbf{M} = \left[\frac{\partial \mathbf{z}}{\partial \boldsymbol{\theta}^T} \ \frac{\partial \mathbf{z}}{\partial \boldsymbol{p}^T} \ \frac{\partial \mathbf{z}}{\partial \boldsymbol{\upsilon}^T} \ \frac{\partial \mathbf{z}}{\partial \sigma^2}\right]. \quad (59)$$

Different kinds of model errors result in different $\mathbf{M}$. We focus on the mutual coupling and gain and phase errors, each parts of matrix $\mathbf{M}$ can be written as:

$$\frac{\partial \mathbf{z}}{\partial \boldsymbol{\theta}^T} = \mathbf{A}_\theta^* \boxdot \mathbf{A} + \mathbf{A}^* \boxdot \mathbf{A}_\theta \quad (60a)$$

$$\frac{\partial \mathbf{z}}{\partial \mathbf{p}^T} = \mathbf{A}^* \boxdot \mathbf{A} \quad (60b)$$

$$\frac{\partial \mathbf{z}}{\partial \boldsymbol{\upsilon}^T} = \mathbf{Q} \quad (60c)$$

$$\frac{\partial \mathbf{z}}{\partial \sigma^2} = \mathrm{vec}(\mathbf{I}_M) \quad (60d)$$

where,

$$\mathbf{A}_\theta = \left[\frac{\partial \mathbf{a}(\theta_1)}{\partial \theta_1}, \frac{\partial \mathbf{a}(\theta_2)}{\partial \theta_2}, \cdots, \frac{\partial \mathbf{a}(\theta_P)}{\partial \theta_P}\right] \quad (61a)$$

$$\mathbf{Q} = \left[\mathbf{G}_1 | \mathbf{G}_2 | \cdots | \mathbf{G}_p\right] \cdot \mathbf{A}(\theta)\mathbf{p} \quad (61b)$$

with

$$\mathbf{G}_p = \frac{\partial \mathbf{C}'}{\partial \boldsymbol{\upsilon}_p}. \quad (62)$$

The partial derivate of vector $\mathbf{z}$ to $\boldsymbol{\theta}$, $\mathbf{p}$, and σ^2 have been developed in study [26]. We only provide the proof of partial derivate to $\boldsymbol{\upsilon}$, i.e., $\frac{\partial \mathbf{z}}{\partial \boldsymbol{\upsilon}^T}$.

Proof: According to the previous discussion, the vector $\mathbf{z}$ can be written as the sum of free-disturb component and disturbance component

$$\mathbf{z} = \mathbf{A}\mathbf{p} + \mathbf{Q}\boldsymbol{\upsilon} + \sigma^2 \mathbf{1}_\mathbf{n}. \quad (63)$$

Only the second part, i.e., $\mathbf{Q}\boldsymbol{\upsilon}$ is the function of vector $\boldsymbol{\upsilon}$, the rest parts is constant for $\boldsymbol{\upsilon}$. As the definition, the partial derivate of vector $\mathbf{z}$ to $\boldsymbol{\upsilon}$ can be written as

$$\frac{\partial \mathbf{z}}{\partial \boldsymbol{\upsilon}^T} = \frac{\partial (\mathbf{Q}\boldsymbol{\upsilon})}{\partial \boldsymbol{\upsilon}^T} \quad (64a)$$

$$= \mathbf{Q}. \quad (64b)$$

Matrix $\mathbf{Q}$ is defined in (61b), for mutual coupling, the matrix $\mathbf{C}'$ is given by (12), while, for gain and phase errors, the matrix $\mathbf{C}'$ is defined by (26). Once, we obtain the FIM, the CRB of DoA estimates can be obtained by inverting the FIM. □

VI. SIMULATION

In this section, we show the robustness of our model when there exist mutual coupling, gain and phase errors, and elements locations errors. However, we only provide simulations for these three kinds of model errors separately. Meanwhile, the uncorrected method, e.g., spatial smoothing MUSIC (SS-MUSIC) [15], [16], and SBL based method [29] are included as references, where SS-MUSIC is used for spectrum comparison, and SBL based method is used for statistical performance comparison. Both nested array and Co-Prime array are examined by simulations. The locations set of the nested array is given by $\mathbb{D} = [1, 2, 3, 4, 8, 12] \cdot \Delta d$ with $\Delta d = \lambda/2$, and the locations set of the Co-Prime array is given by $\mathbb{D} = [0, 2, 3, 4, 6, 9] \cdot \Delta d$. The spatial scope is sampled from $-90°$ to $90°$ with $1°$ being sample interval. The root mean square error (RMSE) is used as the performance metric which is defined as

$$\mathrm{RMSE} = \sqrt{\frac{1}{N_c P}\sum_{i=1}^{P}\sum_{n=1}^{N_c}(\hat{\theta}_{i,n} - \theta_{i,n})^2} \quad (65)$$

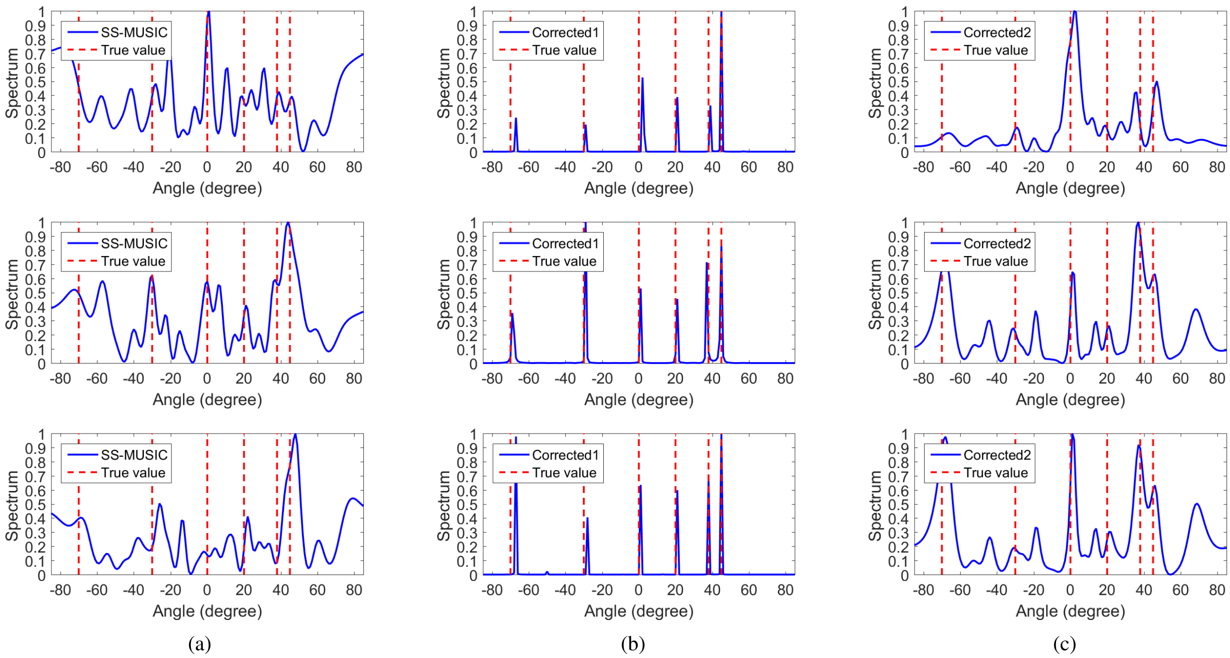

FIGURE 1. Spectra of SS-MUSIC and our method via imperfect 6 elements nested array. The columns (a), (b), and (c) show spectra obtained via SS-MUSIC, corrected estimator based on SBAC (Corrected1), and eigenstructure based estimator(Corrected2), respectively. From top to bottom of each column corresponds to the spectra obtained in the presence of mutual coupling, gain and phase errors, and elements locations error. (a) SS-MUSIC. (b) Corrected1. (c) Corrected2.

where N_c is the number of Monte Carlo trials, P is the number of sources, $\hat{\theta}_{i,n}$ and $\theta_{i,n}$ are the estimates and the true values, respectively.

Fig. 1 shows the spectra obtained via the data collected by the nested array by means of reference method and our methods, where the group (a)-(c) corresponding to the spectra obtained via SS-MUSIC, corrected estimator based on SBAC, and eigenstructure (or ML) based estimator, respectively. The eigenstructure (or ML) based estimator means that the error coefficients and DoAs are estimated jointly based on the models (14), (18), and (43), by means of eigenstructure based gain phase and mutual coupling calibration methods proposed in [6], and ML based sensor location errors correction method proposed in [30]. The results of SBAC based methods are marked by "Corrected1", and the result of eigenstructure (or ML) based corrected estimators are marked by "Corrected2". From top to bottom, each group corresponds to the spectra in the presence of mutual coupling, gain and phase errors, and sensor location errors, respectively. The SNR and number of snapshots are set as 10 dB and 300 separately. Six uncorrelated signals impinge from directions $\boldsymbol{\theta} = [-70°, -30°, 0°, 20°, 38°, 45°]$, and a 6-element nested array is adopted. The model error coefficients are set as

- Mutual coupling coefficients
  $\mathbf{c} = [1, 0.21 + 0.17i, 0.10 + 0.06i]$
- Gain errors $\boldsymbol{\eta} = [0, 0.075, -0.15, 0.1, 0.125, -0.1]$
  Phase errors $\boldsymbol{\phi} = [0°, -4°, -6°, -8°, 7°, 5°]$
- Locations errors
  $\Delta\mathbf{d} = [0, -0.04, 0.06, 0.08, 0.02, -0.06] \cdot \lambda/2$

We can find that SS-MUSIC fails to resolve these sources when there exist model errors. Actually, the model errors destroy the orthogonality between noise subspace and the signal subspace. The SBAC based corrected estimator corresponding to the group (b) can separate these sources successfully with only 6 sensors. The spectrum lines in group (b) confirm that the SBAC based corrected estimators keep the ability of DoF enhancement. The group (c) shows the spectra obtained by means of the eigenstructure (or ML) based corrected estimators. The eigenstructure (for mutual coupling and gain and phase errors), and ML (for sensor location errors) based corrected estimators outperform SS-MUSIC, however, have worse performances than SBAC based corrected estimators. The estimates of error coefficients can be obtained via (52), (53), and (57). As an example of error coefficients estimation result, Table 1 shows the true values and estimates of gains and phases of RF chains and locations. It can be concluded from Table 1 that the gains and phases perturbations and the locations are calibrated effectively, the same trend of mutual coupling coefficients are shown in Table 2

The RMSEs of the DoA estimates versus SNR in the presence of mutual coupling, gain and phase errors, and sensor location errors are shown in the next three paraphrases, respectively. In the simulations, the number of snapshots is fixed to 90. The SNR increases form -20 dB to 13 dB with a step of 3 dB, and 1000 trials are carried out for each value. Two narrow-band uncorrelated sources induce from directions of 38° and 45°. The results and the error coefficients setting are same as above.

TABLE 1. Gain and phase and locations estimation result.

Gain and phase		Locations	
True value	Estimates	True value	Estimates
1	1	1	1
1.072 − 0.074i	1.057 − 0.105i	2.040	2.036
0.845 + 0.089i	0.826 + 0.079i	3.060	3.052
1.089 − 0.153i	1.040 − 0.199i	4.080	4.071
1.117 + 0.137i	1.114 + 0.099i	8.020	8.013
0.896 − 0.078i	0.905 − 0.103i	12.060	12.045

TABLE 2. Mutual coupling estimation result.

True value	Estimates
1	1
0.210 + 0.170i	0.194 + 0.124i
0.100 + 0.060i	0.118 + 0.044i

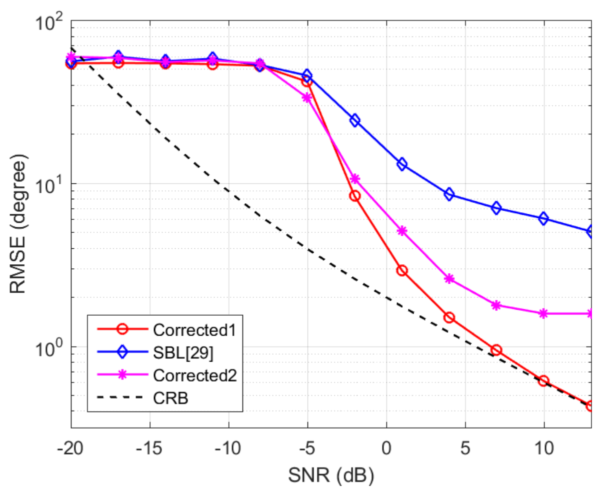

FIGURE 2. RMSE of DoA estimates via nested array versus SNR in the presence of mutual coupling. "Corrected1" corresponds to the result obtained via SBAC based estimator, "Corrected2" denotes to the result obtained via eigenstructure based estimator.

Fig. 2 shows RMSEs of the DoA estimates versus SNR obtained via the nested array in the presence of mutual coupling. A 6-element nested array is adopted. The uncorrected SBL based DoA estimator [29] is adopted as reference. Two kinds of corrected estimators, i.e., the SBAC based estimator and eigenstructure based estimator are examined in this simulation. The dotted line represents the CRB of DoA estimates in presence of mutual coupling. We can find that the SBAC based estimator outperforms uncorrected SBL estimator as well as eigenstructure based corrected estimator. Meanwhile, with the increase of SNR, RMSE of the DoA estimation becomes closer to the CRB. The eigenstructure based corrected estimator also outperforms uncorrected SBL based estimator when SNR is higher than −5 dB.

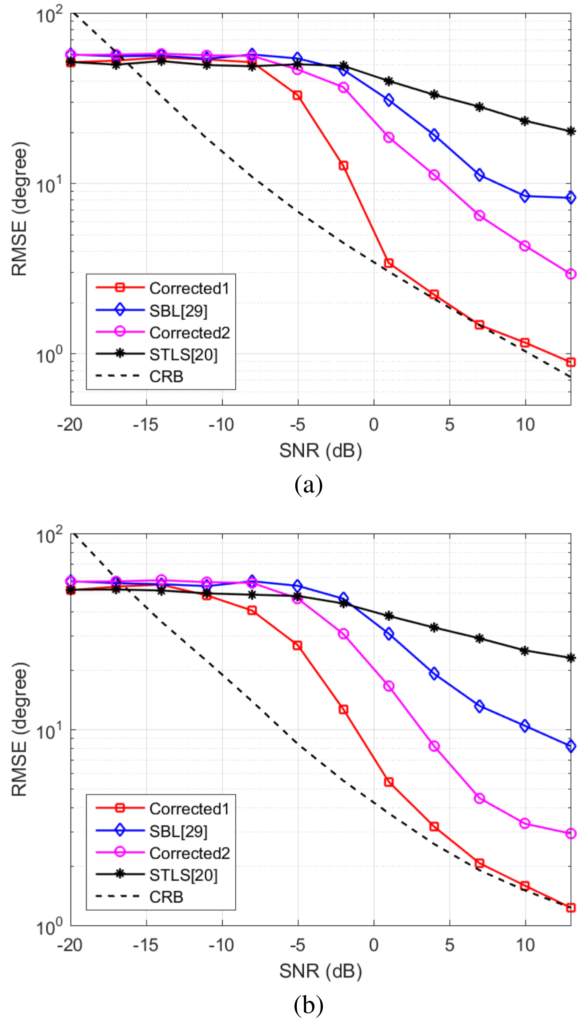

FIGURE 3. RMSE of DoA estimates versus SNR in the presence of gain and phase errors. (a) Nested array, (b) Co-prime array. "Corrected1" corresponds to the result obtained via SBAC based estimator, "Corrected2" denotes to the result obtained via eigenstructure based estimator.

Fig. 3 shows RMSEs of the DoA estimates via two sparse arrays, i.e., nested array and Co-Prime array, in the presence of gain and phase errors. The gain and phase errors coefficients are given by vectors $\boldsymbol{\eta}$ and $\boldsymbol{\phi}$, which are shown in paragraph 2 of this section. For gain and phase errors calibration, Han *et al.* [20] proposed a method named STLS. In this simulation, STLS together with uncorrected SBL based methods are adopted as references, marked as diamond and asterisk, receptively. Similarly, the SBAC based method which is described in Section IV together with eigenstructure based method [6] are examined. The RMSE curves of these two methods are marked by square and circle respectively. We can find from Fig. 3 (a) that SBAC based corrected method has the lowest RMSE curve. Moreover, it becomes closer to CRB with the increase of SNR. The RMSE of eigenstructure based corrected method is higher than SBAC based method, while lower than uncorrected SBL based method and STLS.

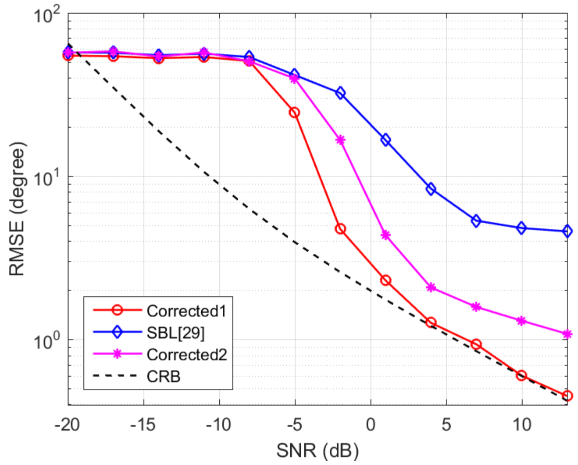

(a)

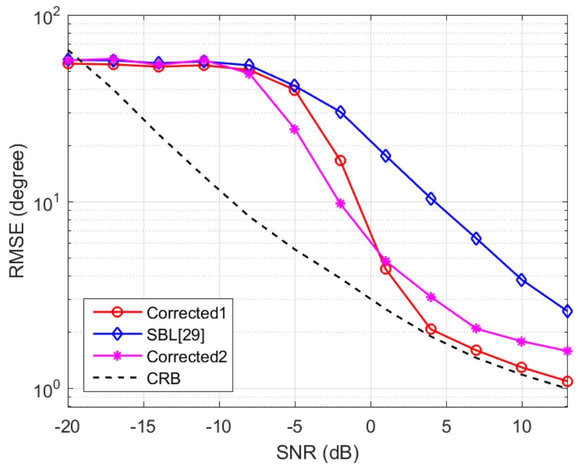

(b)

FIGURE 4. RMSE of DoA estimates versus SNR in the presence of locations errors. (a) Nested array, (b) Co-prime array. "Corrected1" corresponds to the result obtained via SBAC based estimator, "Corrected2" denotes to the result obtained via ML based estimator.

Fig. 3 (b) shows the RMSE curves of these methods based on Co-prime array. The RMSE curves of Co-prime array show the similar trend as the nested array, the difference is that each curve of Co-prime array is slightly higher than corresponding curve of nested array. Because, the virtual ULA of 6 elements nested array is larger than 6-element Co-prime array.

Fig. 4 shows RMSEs of the DoA estimates versus SNR via nested array and Co-prime array with locations errors. The locations errors are given by the vector $\Delta\mathbf{d}$, which is shown in paragraph 2 of this section. The SBAC based corrected method and ML based corrected method [8] are examined in this simulation, meanwhile, the uncorrected SBL based methods is adopt as reference. The RMSE curve of SBAC based method is marked by circle, and ML based corrected method is marked by asterisk. We can find from Fig. 4(a) that the RMSE of SBAC based method outperforms uncorrected SBL based method when the SNR larger than -5 dB. Meanwhile, the ML based corrected estimator outperforms the uncorrected SBL based method. Fig. 4(b) shows the RMSE of DoA estimates based on the Co-prime array. In this case, SBAC based corrected estimator outperforms ML based estimator when the SNR is higher than 0 dB.

VII. CONCLUSION

This paper studied the problem of DoA estimation via Coarray in the presence of model errors, i.e., mutual coupling, gain and/or phase errors, and sensor location errors. The models of the single type error have been established. It is shown that the imperfect Coarray still has the ability of DoF enhancement. The problem of Coarray calibration has been transformed into that of imperfect virtual ULA correction. The effect error matrices of virtual ULA, such as MCM, gain and phase errors matrix, and errors matrix caused by locations perturbation can be expressed analytically by corresponding error coefficients of the Coarray. Therefore, state-of-the-art error correction algorithms can be applied to estimate the unknown error coefficients and DoA based on these models. SBAC is adopted as an example of these methods to estimate DoA and error coefficients jointly in this paper. Simulation results illustrate the effectiveness of our methods for single kind of model error, and the problem of mixed model errors calibration will be studied in future work.

APPENDIX A
STATEMENT OF LEMMA 1

Theorem 1: For $M \times M$ matrix $\mathbf{C}$ and $M \times P$ matrix $\mathbf{A}$, the following relationship holds [28]:

$$(\mathbf{CA})^* \boxdot (\mathbf{CA}) = \mathbf{C}'\mathbf{A}' \tag{66}$$

where

$$\begin{aligned}\mathbf{C}' &= \mathbf{C}^* \otimes \mathbf{C}\\ \mathbf{A}' &= \mathbf{A}^* \boxdot \mathbf{A}\end{aligned}$$

APPENDIX B
ITERATION STEPS OF SBAC

It's hardly achievable to perform straightforward maximization of the density function (51) due to its high nonlinearity. However, Expectation-Maximization(EM) algorithm is very popular to develop an iterative solution for similar problems. Each iteration of the EM algorithm consists of an E-step and an M-step. In the E-step, calculating the expectation of the complete probability $p(\mathbf{z}|\mathbf{p};\boldsymbol{\upsilon},\sigma^2,\boldsymbol{\gamma})$. In the M-step, maximizing the expectation calculated in E-step over the parameters $\mathbf{p}$, $\boldsymbol{\upsilon}$, and σ, by setting the partial derivative for each variable to zeros, we get [27]

$$\boldsymbol{\upsilon} = \left\langle \mathbf{Q}^H\mathbf{Q}\right\rangle^{-1}\left\langle \mathbf{Q}^H\left(\mathbf{z}-\mathbf{Ap}\right)\right\rangle \tag{68a}$$

$$\sigma^2 = \frac{1}{M}\left\langle ||\mathbf{z}-\mathbf{A}'\mathbf{p}||_2^2\right\rangle \tag{68b}$$

$$\boldsymbol{\gamma}_l = \left\langle ||\mathbf{p}_l||_2^2\right\rangle \tag{68c}$$

where $\langle\cdot\rangle$ is conditional expectation under the provability density of $p(\mathbf{p}|\mathbf{z};\boldsymbol{\upsilon},\sigma^2,\boldsymbol{\gamma})$. All three update equations obtain the conditional expectation, which can be obtained further via [27]

$$\left\langle \mathbf{Q}^H\mathbf{Q}\right\rangle_{p_1,p_2} = \mathrm{tr}\left[\mathbf{G}_{p1}^H\mathbf{G}_{p2}\Phi(\boldsymbol{\mu}\boldsymbol{\mu}^H + \boldsymbol{\Sigma}_\mathbf{p})\right] \tag{69a}$$

$$\left\langle \mathbf{Q}^H\mathbf{z}\right\rangle_{p} = \mathrm{tr}\left[\mathbf{G}_{p}^H\mathbf{z}\boldsymbol{\mu}^H\Phi\right] \tag{69b}$$

$$\left\langle \mathbf{Q}^H\mathbf{A}\mathbf{p}\right\rangle_{p} = \mathrm{tr}\left[\mathbf{G}_{p}^H\mathbf{A}(\boldsymbol{\mu}\boldsymbol{\mu}^H + \boldsymbol{\Sigma}_\mathbf{p})\boldsymbol{\Phi}\right] \tag{69c}$$

$$\left\langle ||\mathbf{z}-\mathbf{A}'\mathbf{p}||_2^2\right\rangle = \nu||\mathbf{z}-\mathbf{A}'\boldsymbol{\mu}||_2^2 + \mathrm{tr}\left[\mathbf{A}'\boldsymbol{\Sigma}_\mathbf{p}(\mathbf{A}')^H\right] \tag{69d}$$

where

$$\boldsymbol{\mu} = \boldsymbol{\Gamma}(\mathbf{A}')^H\boldsymbol{\Sigma}_\mathbf{p}^{-1}\mathbf{z} \tag{70a}$$

$$\boldsymbol{\Sigma}_\mathbf{p} = \boldsymbol{\Gamma} - \boldsymbol{\Gamma}(\mathbf{A}')^H\boldsymbol{\Sigma}_\mathbf{z}^{-1}\mathbf{p}\mathbf{A}'\boldsymbol{\Gamma} \tag{70b}$$

$$\boldsymbol{\Sigma}_\mathbf{z} = \sigma^2\mathbf{I}_M + \mathbf{A}'\boldsymbol{\Gamma}(\mathbf{A}')^H \tag{70c}$$

The final updating equation can obtained by substituting (69) and (70) into (68). After the convergence of iteration, the estimation of $\mathbf{p}$ will be given by $\hat{\mathbf{p}} = \boldsymbol{\mu}$.

REFERENCES

[1] K. Guan et al., "On millimeter wave and THz mobile radio channel for smart rail mobility," IEEE Trans. Veh. Technol., vol. 66, no. 7, pp. 5658–5674, Jul. 2017.
[2] X. Chen, M. Zhang, S. Zhu, and A. Zhang, "Empirical study of angular-temporal spectra in a reverberation chamber," IEEE Trans. Antennas Propag., to be published. [Online]. Available: https://ieeexplore.ieee.org/document/8429904, doi: 10.1109/TAP.2018.2864343.
[3] R. O. Schmidt, "Multiple emitter location and signal parameter estimation," IEEE Trans. Antennas Propag., vol. 34, no. 3, pp. 276–280, Mar. 1986.
[4] R. Roy and T. Kailath, "Esprit-estimation of signal parameters via rotational invariance techniques," IEEE Trans. Acoust., Speech, Signal Process., vol. 37, no. 7, pp. 984–995, Jul. 1989.
[5] X. Chen, S. Zhang, and Q. Li, "A review of mutual coupling in MIMO systems," IEEE Access, vol. 6, pp. 24706–24719, 2018.
[6] B. Friedlander and A. J. Weiss, "Direction finding in the presence of mutual coupling," IEEE Trans. Antennas Propag., vol. 39, no. 3, pp. 273–284, Mar. 1991.
[7] A. J. Weiss and B. Friedlander, "Eigenstructure methods for direction finding with sensor gain and phase uncertainties," Circuits Syst. Signal Process., vol. 9, no. 3, pp. 271–300, 1990.
[8] A. J. Weiss and B. Friedlander, "Array shape calibration using sources in unknown locations-a maximum likelihood approach," IEEE Trans. Acoust., Speech, Signal Process., vol. 37, no. 12, pp. 1958–1966, Dec. 1989.
[9] F. Sellone and A. Serra, "A novel online mutual coupling compensation algorithm for uniform and linear arrays," IEEE Trans. Signal Process., vol. 55, no. 2, pp. 560–573, Feb. 2007.
[10] J. Dai, D. Zhao, and X. Ji, "A sparse representation method for DOA estimation with unknown mutual coupling," IEEE Antennas Wireless Propag. Lett., vol. 11, pp. 1210–1213, 2012.
[11] P. Rocca, M. A. Hannan, M. Salucci, and A. Massa, "Single-snapshot DoA estimation in array antennas with mutual coupling through a multiscaling BCS strategy," IEEE Trans. Antennas Propag., vol. 65, no. 6, pp. 3203–3213, Jun. 2017.
[12] M. Hawes, L. Mihaylova, F. Septier, and S. Godsill, "Bayesian compressive sensing approaches for direction of arrival estimation with mutual coupling effects," IEEE Trans. Antennas Propag., vol. 65, no. 3, pp. 1357–1368, Mar. 2017.
[13] Q. Wang, T. Dou, H. Chen, W. Yan, and W. Liu, "Effective block sparse representation algorithm for DOA estimation with unknown mutual coupling," IEEE Commun. Lett., vol. 21, no. 12, pp. 2622–2625, Dec. 2017.
[14] H. Wu, C. Hou, H. Chen, W. Liu, and Q. Wang, "Direction finding and mutual coupling estimation for uniform rectangular arrays," Signal Process., vol. 117, pp. 61–68, Dec. 2015.
[15] P. Pal and P. P. Vaidyanathan, "Nested arrays: A novel approach to array processing with enhanced degrees of freedom," IEEE Trans. Signal Process., vol. 58, no. 8, pp. 4167–4181, Aug. 2010.
[16] P. Pal and P. P. Vaidyanathan, "Coprime sampling and the MUSIC algorithm," in Proc. 14th IEEE DSP/SPE Workshop, Sedona, AZ, USA, Jan. 2011, pp. 289–294.
[17] M. Wang and A. Nehorai, "Coarrays, MUSIC, and the Cramér–Rao bound," IEEE Trans. Signal Process., vol. 65, no. 4, pp. 933–946, Feb. 2017.
[18] Q. Shen, W. Liu, W. Cui, and S. Wu, "Underdetermined DOA estimation under the compressive sensing framework: A review," IEEE Access, vol. 4, pp. 8865–8878, Nov. 2016.
[19] J. Cai, W. Liu, R. Zong, and B. Wu, "Sparse array extension for non-circular signals with subspace and compressive sensing based DOA estimation methods," Signal Process., vol. 145, pp. 61–68, Apr. 2018.
[20] K. Han, P. Yang, and A. Nehorai, "Calibrating nested sensor arrays with model errors," IEEE Trans. Antennas Propag., vol. 63, no. 11, pp. 4739–4748, Nov. 2015.
[21] C. L. Liu and P. P. Vaidyanathan, "Super nested arrays: Linear sparse arrays with reduced mutual coupling—Part II: High-order extensions," IEEE Trans. Signal Process., vol. 64, no. 16, pp. 4203–4217, Aug. 2016.
[22] C. L. Liu and P. P. Vaidyanathan, "Super nested arrays: Linear sparse arrays with reduced mutual coupling—Part I: Fundamentals," IEEE Trans. Signal Process., vol. 64, no. 15, pp. 3997–4012, Aug. 2016.
[23] J. Liu, Y. Zhang, Y. Lu, S. Ren, and S. Cao, "Augmented nested arrays with enhanced DOF and reduced mutual coupling," IEEE Trans. Signal Process., vol. 65, no. 21, pp. 5549–5563, Nov. 2017.
[24] C. L. Liu and P. P. Vaidyanathan, "Hourglass arrays and other novel 2-D sparse arrays with reduced mutual coupling," IEEE Trans. Signal Process., vol. 65, no. 13, pp. 3369–3383, Jul. 2017.
[25] T. Basikolo, K. Ichige, and H. Arai, "A novel mutual coupling compensation method for underdetermined direction of arrival estimation in nested sparse circular arrays," IEEE Trans. Antennas Propag., vol. 66, no. 2, pp. 909–917, Feb. 2018.
[26] M. Wang, Z. Zhang, and A. Nehorai, "Performance analysis of coarray-based MUSIC in the presence of sensor location errors," IEEE Trans. Signal Process., vol. 66, no. 12, pp. 3074–3085, Jun. 2018.
[27] Z.-M. Liu and Y.-Y. Zhou, "A unified framework and sparse Bayesian perspective for direction-of-arrival estimation in the presence of array imperfections," IEEE Trans. Signal Process., vol. 61, no. 15, pp. 3786–3798, Aug. 2013.
[28] H. L. Van Trees, Optimum Array Processing: Part IV of Detection, Estimation, and Modulation Theory. Hoboken, NJ, USA: Wiley, 2004.
[29] D. P. Wipf and B. D. Rao, "Sparse Bayesian learning for basis selection," IEEE Trans. Signal Process., vol. 52, no. 8, pp. 2153–2164, Aug. 2004.
[30] B. C. Ng and C. M. S. See, "Sensor-array calibration using a maximum-likelihood approach," IEEE Trans. Antennas Propag., vol. 44, no. 6, pp. 827–835, Jun. 1996.

RUI LU received the B.Eng. degree in information engineering from Xi'an Jiaotong University, Xi'an, China, in 2014, where he is currently pursuing the Ph.D. degree in electronics science and technology.

His research interests include array signal processing, compressive sensing, and its application for direction-of-arrival estimation and channel estimation.

MING ZHANG received the B.S. and M.S. degrees in information and communication engineering and the Ph.D. degree in electronic science and technology from Xi'an Jiaotong University, Xi'an, China, in 2008, 2011, and 2017, respectively.

From 2011 to 2014, he was with the Antenna and Propagation Research Center, Huawei Technologies Co., Ltd. From 2014 to 2017, he was with the Communication and Navigation Department, AVIC Avionics Co., Ltd. He is currently a Post-Doctoral Researcher with the School of Electronic and Information Engineering, Xi'an Jiaotong University. His research interests include adaptive filtering, spectrum estimation, and beamforming, with applications to radar, wireless communications, and satellite navigations.

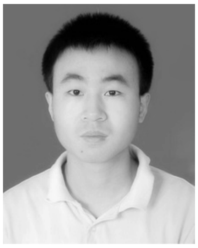

XIAOBO LIU received the B.Eng. degree in information engineering from Xi'an Jiaotong University, Xi'an, China, in 2014, where he is currently pursuing the Ph.D. degree in electronics science and technology.

His research interests include metasurface, design of antenna, microwave circuit, and electromagnetic theory.

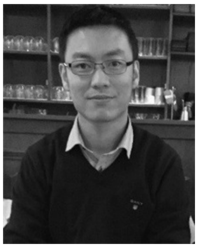

XIAOMING CHEN (M'16) received the B.Sc. degree in electrical engineering from Northwestern Polytechnical University, Xi'an, China, in 2006, and the M.Sc. and Ph.D. degrees in electrical engineering from the Chalmers University of Technology, Gothenburg, Sweden, in 2007 and 2012, respectively.

From 2013 to 2014, he was a Post-Doctoral Researcher with the Chalmers University of Technology. From 2014 to 2017, he was an Antenna Specialist with Qamcom Research & Technology AB, Gothenburg. Since 2017, he has been a Professor with Xi'an Jiaotong University, Xi'an. His research areas include MIMO antennas, over-the-air testing, reverberation chambers, and hardware impairments and mitigation.

Dr. Chen was a recipient of the 1000-Talent Plan for Young Scholars in China. He received the International Union of Radio Science Young Scientist Awards in 2017 and 2018. He serves as an Associate Editor for the IEEE Antennas and Wireless Propagation Letters and received the Outstanding Associate Editor Award in 2018.

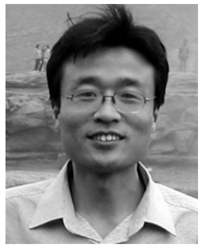

ANXUE ZHANG received the B.S. degree in electrical and electronics engineering from Henan Normal University, Xinxiang, China, in 1996, and the M.S. and Ph.D. degrees in electromagnetic and microwave engineering from Xi'an Jiaotong University, Xi'an, China, in 1999 and 2003, respectively.

He is currently a Professor with Xi'an Jiaotong University. His current research interests include antenna design, radio-frequency and microwave circuit design, array signal processing, and metamaterials.